

Sensors

A Triphenyl Amine-Based Solvatofluorochromic Dye for the Selective and Ratiometric Sensing of OCI^- in Human Blood Cells

Shyamaprosad Goswami,^{*,[a]} Krishnendu Aich,^[a] Sangita Das,^[a] Bholanath Pakhira,^[a] Kakali Ghoshal,^[b] Ching Kheng Quah,^[c] Maitree Bhattacharyya,^[b] Hoong-Kun Fun,^[c, d] and Sabyasachi Sarkar^[a]

Abstract: A new visible-light-excitable fluorescence ratiometric probe for OCI^- has been developed based on a triphenylamine-diaminomaleonitrile (TAM) moiety. The structure of the dye was confirmed by single-crystal X-ray analysis. It behaves as a highly selective and sensitive probe for OCI^- over other analytes with a fast response time (~ 100 s). OCI^- reacts with the probe leading to the formation of the corresponding aldehyde in a mixed-aqueous system. The detection limit of the probe is in the 10^{-8} M range. The probe

(TAM) also exhibits solvatofluorochromism. Changing the solvent from non-polar to polar, the emission band of TAM largely red-shifted. Moreover, the probe shows an excellent performance in real-life application in detecting OCI^- in human blood cells. The experimentally observed changes in the structure and electronic properties of the probe after reaction with OCI^- were studied by DFT and TDDFT computational calculations.

Introduction

Hypochlorous acid is one of the most potent toxic chemicals in biology.^[1] The highly active free acid gets dissociated at the biological pH as hypochlorite ion.^[2] Unlike most of the other reactive oxygen species (ROS) and reactive nitrogen species (RNS), the hypochlorite anion (OCI^-) is widely used in our daily life. Hypochlorite has been extensively used as a bleaching agent, disinfectant in water purification, cooling-water treatment as well as in the removal of cyanide. Hypochlorite is endogenously produced in the body by peroxidation of chloride ions catalyzed by myeloperoxidase (MPO)^[3] in neutrophils.

However, the excessive accumulation of this strong oxidative OCI^- inside the human body is harmful as it can damage host tissue, ultimately causing a wide range of diseases, such as kidney failure,^[4] arthritis,^[5] cancer,^[6] cardiovascular disease,^[7] lung injury,^[8] renal disease,^[9] etc.

Therefore, the development of an easy and affordable detection procedure for hypochlorite/ OCI^- is of great importance to understanding the role of OCI^- in immunization and diseases. In this regard, fluorescence techniques are regarded as a promising tool for the detection of various analytes. To date, a number of fluorescence probes has been reported for the selective detection of OCI^- .^[10] Several probes have been demonstrated to possess a reasonable selectivity of OCI^- over other ROS, but still they have few limitations which may hamper their practical applicability, such as low solubility in water, poor detection limit, and excitation and emission wavelengths in the UV region. For in-vivo imaging, the excitability of the probe in the visible or NIR (near infrared) region is most appropriate to suppress autofluorescence, photobleaching and photodamage of the biological samples. Therefore, there is a critical demand to develop probes that can easily be synthesized, provide a ratiometric response, and have long excitation and emission wavelengths to facilitate in-vivo imaging.^[11]

In continuation of our work on developing new probe materials^[12] we herein report the synthesis as well as photophysical and sensing properties of a Schiff base based on triphenylamine bearing a diaminomaleonitrile moiety. The structure of the probe was supported by single-crystal X-ray study. The probe (TAM) exhibits a ratiometric response in its emission profile after interaction with OCI^- and displayed solvatofluorochromism with varying solvent polarity. Density functional

[a] Prof. S. Goswami, K. Aich, S. Das, B. Pakhira, Prof. S. Sarkar
Department of Chemistry
Indian Institute of Engineering Science and Technology
Shibpur, Howrah-711103 (India)
E-mail: spgoswamical@yahoo.com

[b] K. Ghoshal, Dr. M. Bhattacharyya
Department of Biochemistry
University of Calcutta
Kolkata-700019 (India)

[c] Dr. C. K. Quah, Prof. H.-K. Fun
X-ray Crystallography Unit
School of Physics
Universiti Sains Malaysia
11800 USM, Penang (Malaysia)

[d] Prof. H.-K. Fun
Department of Pharmaceutical Chemistry
College of Pharmacy
King Saud University
Riyadh 11451 (Saudi Arabia)

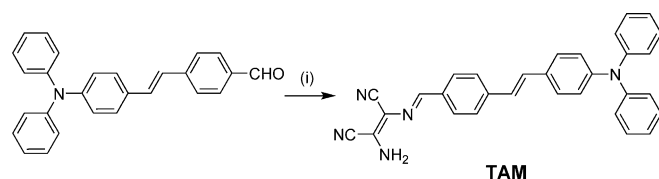
Supporting information for this article is available on the WWW under <http://dx.doi.org/10.1002/asia.201403234>.

theory (DFT) and time-dependent DFT (TDDFT) studies have been performed to understand the sensing mechanism. Moreover, we show that TAM can be used for bio-imaging in human blood cells.

Results and Discussion

Synthesis of the Probe

The synthetic procedure of TAM is shown in Scheme 1. Compound (*E*)-4-(4-diphenylamino)styryl)benzaldehyde was synthesized according to a literature procedure.^[13] In the final step, (*E*)-4-(4-diphenylamino)styryl)benzaldehyde was refluxed with



Scheme 1. Reagents and conditions: (i) diaminomaleonitrile, EtOH, reflux, 12 h.

diaminomaleonitrile in ethanol. The product (TAM) was obtained as a yellow powder, which was characterized by ¹H NMR, ¹³C NMR, HRMS (Supporting Information, Figures S5–S9) and single-crystal X-ray structure.

Crystallographic Studies

A summary of the crystallographic data is given in Table S2 in the Supporting Information. The compound TAM exists in *trans-trans-cis* conformations (Figure 1a) with respect to the C19=C20 [1.357(7) Å], N2=C27 [1.304(6) Å] and C28=C29 bonds [1.388(7) Å]. The dihedral angles between the benzene rings [C1–C6 (A), C7–C12 (B), C13–C18 (C) and C21–C26 (D)] are 62.1(3)° [A/B], 68.6(3)° [A/C], 74.9(3)° [A/D], 60.2(3)° [B/C], 67.0(3)° [B/D] and 7.9(3)° [C/D]. In the crystal packing, adjacent molecules are linked via intermolecular 'head-to-tail' N5–H2N5...N3 hydrogen bonds (Table S3, Supporting Information) into chains propagating in [101] (Figure 1b), forming C(8) motifs which were stacked along [010] (Figure S12a, Supporting Information). These chains (excluding the two terminal benzene rings) model a sheet-like arrangement of molecules (Figure S12b, Supporting Information) and were separated by an interlayer distance of 3.37 Å. The crystal structure is further consolidated by weak C–H...π (Cg1) interactions (Table S3) where Cg1 is the centroid of the C1–C6 benzene ring.

Solvatofluorochromic Behavior

The electronic absorption and emission properties of TAM demonstrate a strong solvent dependence, which can be visually observed. We have used commonly used organic solvents like *n*-hexane, toluene, THF, CH₂Cl₂ and CH₃CN to check such an effect. Fluorescence emission spectra of TAM exhibit a prom-

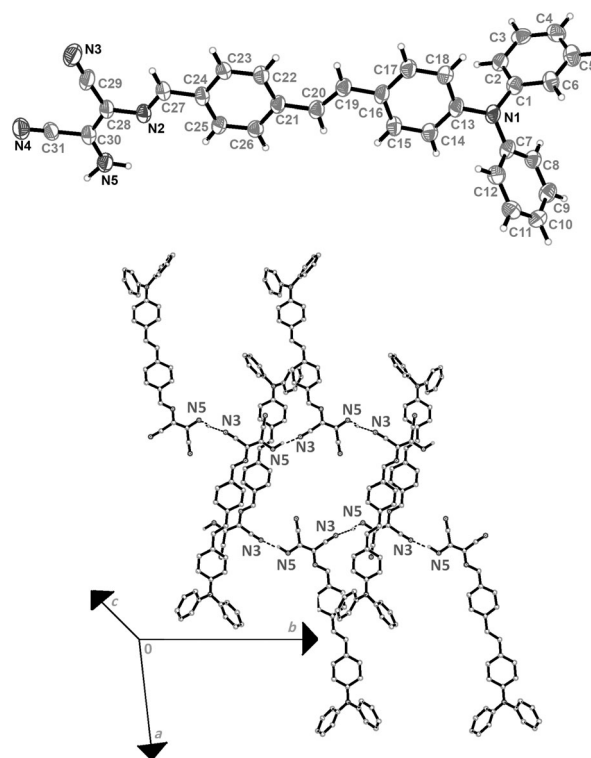


Figure 1. (a) The crystal structure of TAM, showing 50% probability displacement ellipsoids for non-H atoms and the atom-numbering scheme. (b) View showing the C(6) chain motifs running along the [010].

inent solvatofluorochromism (Figure 2a). It was observed that with changing solvent polarity from *n*-hexane to CH₃CN, TAM exhibits changes in fluorescence color under UV light illumination from blue to red (Figure 2b). From non-polar *n*-hexane to polar CH₃CN the emission peak of TAM largely red-shifted from 492 nm to 682 nm. Such color change may be attributed to

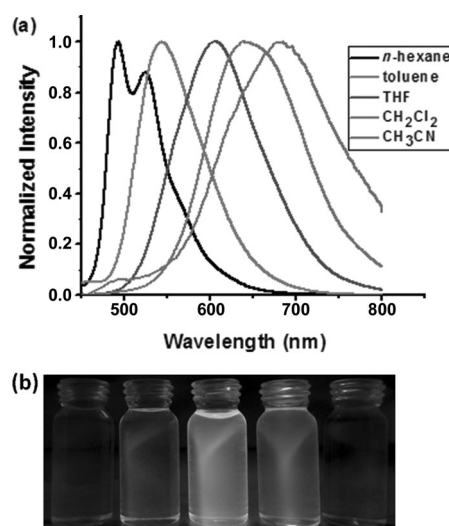


Figure 2. (a) Solvent-dependent emission spectra of TAM (5 μM, λ_{ex} = 430 nm); (b) Photos of TAM solution (5 μM) in different solvents under irradiation with UV light (from left to right: *n*-hexane, toluene, THF, CH₂Cl₂ and CH₃CN).

the presence of a D- π -A structure as the photophysical behavior of D- π -A conjugates depends solely on the solvent polarity. Thus, this probe can be used as a sensitive probe of solvent polarity, and the data obtained are listed in Table S1.

Sensing of OCI^-

UV/Vis studies

In the absence of any guest analytes TAM (10 μM) showed two absorption bands at 430 nm and 305 nm in its electronic spectrum measured in THF/ H_2O (2:3, v/v, 25 $^\circ\text{C}$) solvent. An initial test titration of the receptor TAM with OCI^- showed an immediate change in color from yellow to colorless which was detectable even by the naked eye (Figure 3a). No abrupt change

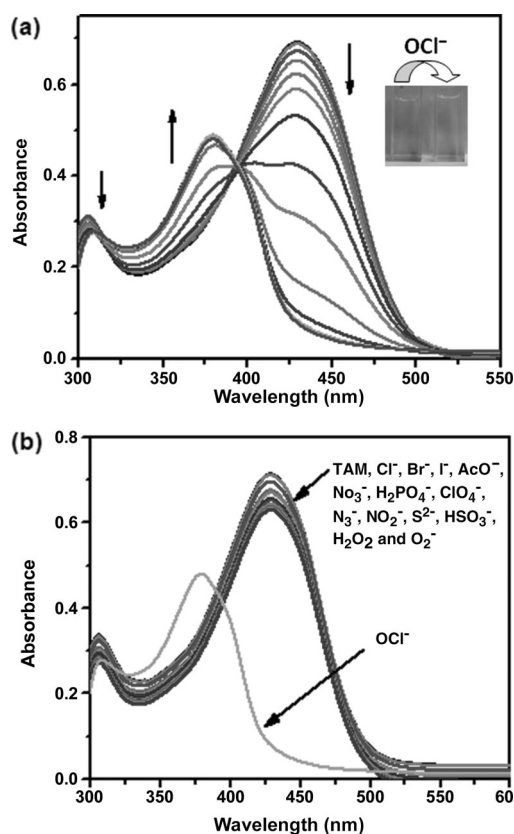


Figure 3. UV/Vis spectra of TAM (10 μM) in THF/ H_2O (2:3, v/v, pH 7.1) in the presence of (a) OCI^- (0–5 equivalents) and (b) different analytes (5 equivalents). Inset: visible color change of TAM upon addition of 2 equivalents of OCI^- in ambient light.

in color was noticed in case of other analytes, such as Cl^- , Br^- , I^- , AcO^- , NO_3^- , H_2PO_4^- , ClO_4^- , N_3^- , NO_2^- , S^{2-} , HSO_3^- (as their sodium salt), H_2O_2 and O_2^- (Figure 3b). These results suggest that the attack at the target center is caused by OCI^- only. The UV/Vis study suggests that TAM can selectively detect OCI^- colorimetrically even in the presence of other competitive analytes as stated above. Upon gradual addition of OCI^- solution (0 to 50 μM) into the solution of TAM (10 μM , THF/ H_2O , 2:3, 25 $^\circ\text{C}$), a new absorption peak slowly appears at 380 nm and the peak at 430 nm gradually decreases with an isosbestic

point at 394 nm. A large blue shift of 100 nm in the absorption spectrum was observed. An intense color change (from yellow to colorless) was observed with the emergence of a new band around at 380 nm in the electronic spectrum, which may be attributed to the formation of a new species.

Fluorescence studies

In the fluorescence spectrum, the free probe TAM (10 μM , THF/ H_2O , 2:3, v/v, pH 7.1, $\Phi = 0.28$) exhibits an emission peak at 630 nm when excited at 430 nm, and no noticeable variations are observed under the assay conditions, suggesting that TAM is a stable molecule. Upon introduction of OCI^- into the solution of TAM, a ratiometric fluorescence change was observed. The peak at 630 nm gradually decreases and a new peak at 485 nm gradually increases (Figure 4a).

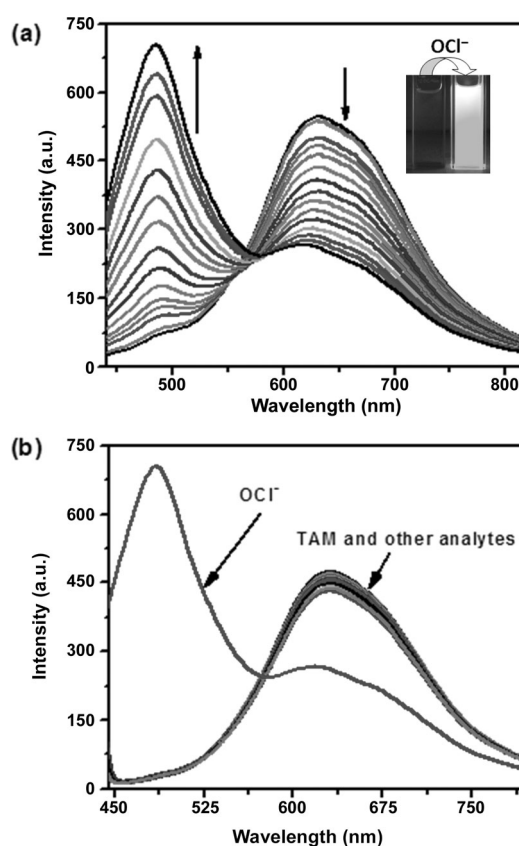


Figure 4. Emission spectra of TAM (10 μM) in THF/ H_2O (2:3, v/v, pH 7.1) in the presence of (a) OCI^- (0–5 equivalents) and (b) different analytes (5 equivalents); $\lambda_{\text{exc}} = 430$ nm. Inset: emission color change of TAM upon addition of 2 equivalents of OCI^- after illumination with UV light.

The fluorescence quantum yield calculated at this stage is 0.86, using fluorescein as a reference ($\Phi = 0.97$ in basic ethanol). A plot of the fluorescent emission ratio (I_{630}/I_{485}) as a function of OCI^- concentration (0–26 μM) showed a linear relationship with an R^2 value of 0.9935 (Figure S2, Supporting Information).

The detection limit of TAM for OCI^- is determined from the emission spectral change, using the equation $\text{DL} = K \times \text{Sb}_1 / \text{S}$,

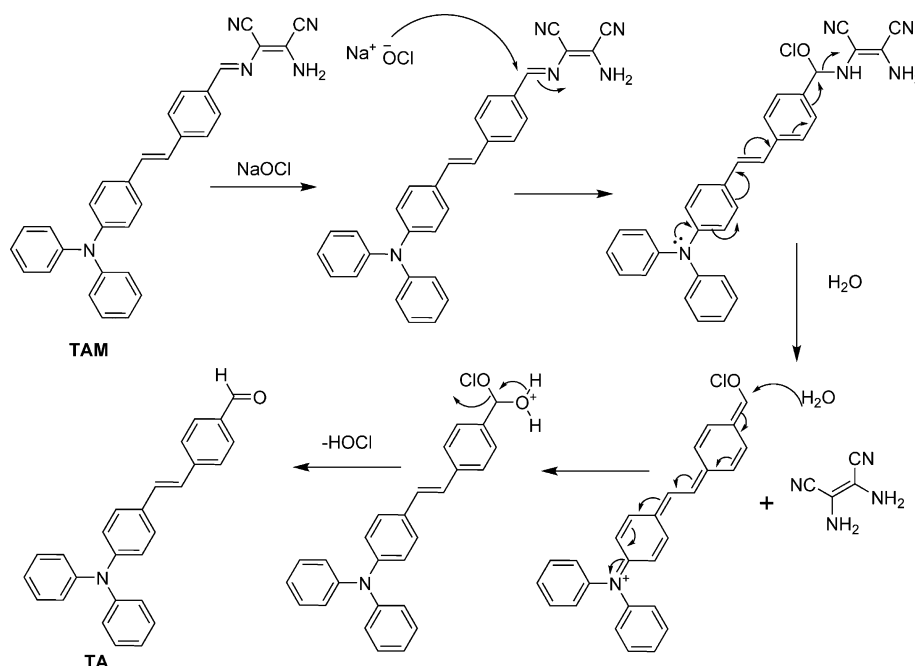
where $K=3$, Sb_1 is the standard deviation of the blank solution, and S is the slope of the calibration curve.^[14] The detection limit was evaluated to be 7×10^{-8} M, indicating that TAM has a very good sensitivity for the detection of OCl^- .

Next, the sensitivity and the selectivity of the receptor TAM towards OCl^- were examined by employing different analytes in aqueous THF solution. TAM shows a strong increase in emission at 485 nm upon addition of OCl^- , whereas no observable change was detected upon addition of other competing anions, thus establishing the selectivity of TAM towards OCl^- (Figure 4b).

The efficiency of a receptor to determine a particular analyte in the presence of other analytes is determined by competition experiments. Here, the interference of other competing anions was also investigated by competition experiments (Figure S4, Supporting Information). When TAM was treated with 2.0 equiv of OCl^- in the presence of other anions at the same concentration, the detection of OCl^- was not hampered, that is, no interference for the detection of OCl^- was observed. Hence, TAM can be used as a selective and sensitive colorimetric as well as fluorogenic ratiometric probe for OCl^- .

In aqueous THF solution, the reaction-based product was hydrolyzed and finally the corresponding aldehyde was produced, whose identity was established by 1H NMR and HRMS spectroscopic analyses (Figure 5 and Figure S10, Supporting Information). The proposed product (TA) was isolated, and it was observed that the product was formed simultaneously. The plausible mechanism of the interaction between TAM and OCl^- is presented in Scheme 2. TAM is first oxidatively attacked by OCl^- to the imino group, which later may lose the diamino-leonitrile unit. This is facilitated by the nucleophilic electron-donating effect of the lone pair on the N atom through extended conjugation that follows the nucleophilic attack by H_2O with the elimination of HOCl forming the TA molecule (Scheme 2).

In the case of chemodosimetric approach, the reaction time plays an important role; therefore, the reaction time required for the interaction between TAM and OCl^- was monitored using similar experimental conditions after the addition of 2 equivalents of OCl^- . As shown in Figure S1, the fluorescence intensity increased rapidly with the reaction time and then leveled off in less than 2 min (~ 100 s). We can conclude from this experiment that our probe is suitable for the rapid detection of OCl^- . A good linear relationship was observed between fluorescence intensity ratio (I_{485}/I_{630}) and reaction time from 0–100 s (Figure S1).



Scheme 2. Possible mechanism of the response of TAM towards hypochlorite (OCl^-).

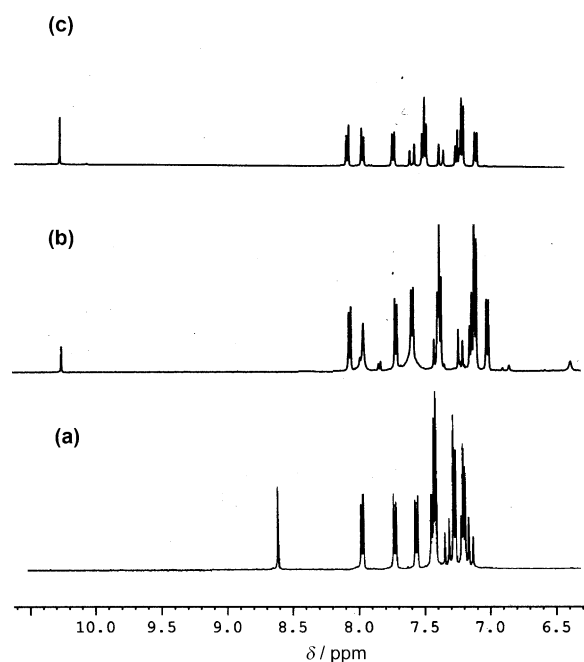


Figure 5. Partial 1H NMR (500 MHz) spectra of (a) TAM, (b) [TAM + OCl^-] and (c) [TA] in $[D_6]DMSO$. [TAM] = [TA] = 2.5×10^{-2} M; $[OCl^-]$ = 1.5×10^{-1} M.

pH study

To examine the pH sensitivity of the probe, we have performed an acid–base titration experiment. TAM does not undergo any notable change in the fluorescence profile within the pH range from 2–10.5. From this observation, we can conclude that the molecule is stable in this pH range. The fluorescence change with different pH is depicted in Figure S16. Now from the above observation we can conclude that TAM can be employed for the detection of OCl^- in a broad pH range.

Sensing of OCI^- using TLC plates

Efforts were made to examine the binding of OCI^- with the receptor TAM in the solid state. In order to investigate a practical application of this probe, so-called “dip-stick” experiments were performed. This simple but very important approach pro-

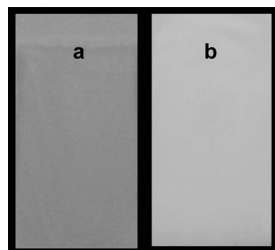


Figure 6. Emission color changes of TAM on a TLC plate in the absence and presence of OCI^- under irradiation with UV light.

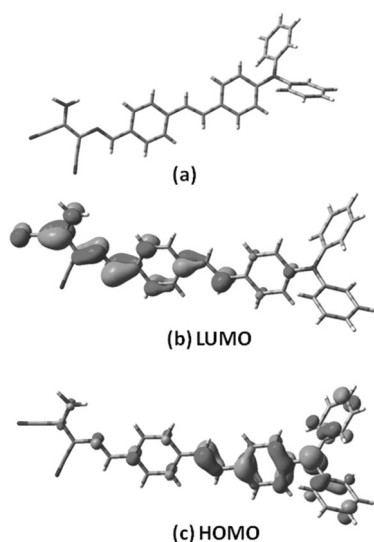


Figure 7. Optimized structures, HOMO and LUMO orbitals of TAM calculated at the DFT level using the B3LYP/6-311G+(d,p) basis set.

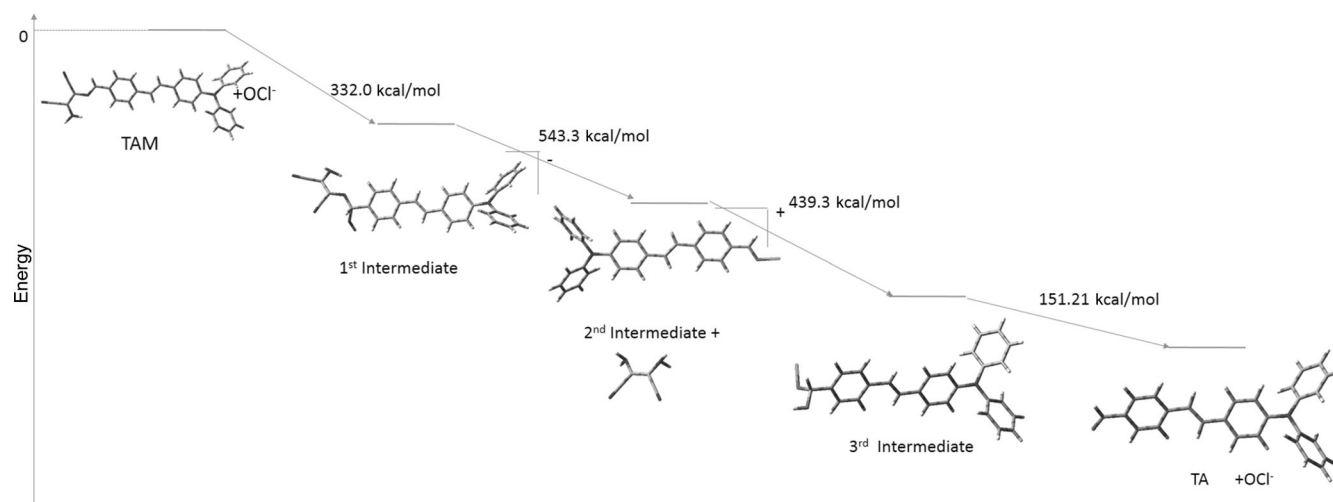


Figure 8. Reaction mechanism with energy changes calculated at the DFT level using the B3LYP/6-311G+(d,p) basis set.

vides instant qualitative information without resorting to instrumental analysis. To this end, a TLC plate was dipped into a solution of TAM (2×10^{-4} M) in THF and then dried in air. To detect OCI^- , we then immersed the TLC plate into OCI^- (2×10^{-4} M) solution, followed again by drying in air to evaporate the solvent. The color of the TLC plates changed from yellowish green to deep bluish green (Figure 6). Hence, the feasibility of real-time monitoring of OCI^- in a qualitative manner without any instrumental analysis but visualization through the naked eye has been demonstrated here.

Computational study

To understand the relationship between the structural changes of TAM to TAM- OCI^- (TA) on addition of OCI^- and their electronic spectra, density functional theory (DFT) and time-dependent density functional theory (TDDFT) calculations with the B3LYP/6-311G+d,p method basis set using the Gaussian 03W, Revision D.01 program was carried out and visualized using Gauss view program. The optimized geometry and the highest occupied molecular orbital (HOMO) and lowest unoccupied molecular orbital (LUMO) of TAM are shown in Figure 7.

For the TD-DFT calculation, solvent correction was incorporated by CPCM model and a 1:1 mixture of water and THF was chosen as the solvent. The calculated absorption spectra show peaks at 432.90 nm ($f=1.0113$) and 329.29 nm ($f=0.0569$) for TAM, which are due to HOMO-1 to LUMO+2 and HOMO to LUMO+2 transitions, respectively. However, for TA, HOMO to LUMO transition is responsible for the absorption at 389.42 nm ($f=1.0089$). The possible interaction between TAM and OCI^- has been investigated using DFT calculation, and each of the probable intermediate state was optimized; the proposed intermediates are listed in Figure 8.

Bioimaging study

TAM is particularly useful for imaging of biological samples owing to its permeability as well as stability. This fluorescent

probe is easily taken up by the cells without causing any damages such as lysis or swelling. Figure 9a,b depicts the bioimaging of human peripheral blood mononuclear cells (PBMCs) by TAM without external addition of OCl^- . Here, cells show signifi-

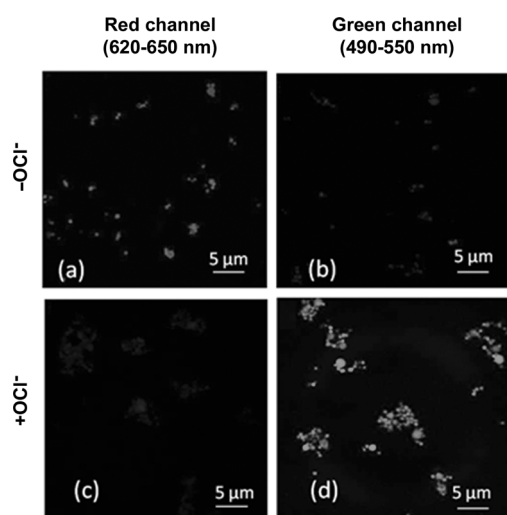


Figure 9. Confocal fluorescence images of human PBMCs treated with $10 \mu\text{M}$ TAM in the absence (a,b) and presence (c,d) of $20 \mu\text{M}$ NaOCl solution; $\lambda_{\text{ex}} = 430 \text{ nm}$.

cant red fluorescence with little or no green fluorescence. The small green autofluorescence may be due to the endogenous OCl^- present within the cells as a reactive oxygen species. Figure 9c,d shows the green fluorescent signals obtained after addition of OCl^- , indicating the interactions between TAM and OCl^- .

The average fluorescence intensity has been calculated by using the Olympus Fluoview FV1000 software, and the result is provided in Table S4 in the Supporting Information. The green/red ratio is significantly lower in samples without added OCl^- (0.233) as compared to that with externally added OCl^- (2.983), thus implicating a shift from red fluorescence to green fluorescence. Accordingly, TAM has been shown to be a successful probe for bioimaging.

Conclusions

In summary, we have demonstrated a novel ratiometric fluorescent probe capable of selective detection of hypochlorite in a mixed aqueous medium. The structure of the probe was confirmed by single-crystal X-ray analysis. The reaction mechanism between the probe and OCl^- has been established by ^1H NMR spectroscopic and mass spectral data. Moreover, this fluorescent dye exhibits a solvatochromic effect in different polar solvents. The spectroscopic studies were further supported by DFT and TDDFT calculations. The detection limit of our probe is in the 10^{-8} M range. The potential of the probe for practical application was confirmed by employing it for fluorescence bioimaging in human blood cells.

Experimental Section

General

Unless otherwise mentioned, materials were obtained from commercial suppliers and were used without further purification. Thin layer chromatography (TLC) was carried out using Merck 60 F_{254} plates with a thickness of 0.25 mm. Melting points were determined on a hot-plate melting point apparatus in an open-mouth capillary and are uncorrected. ^1H and ^{13}C NMR spectra were recorded on Bruker 500 MHz and 125 MHz instruments, respectively. For NMR spectra, CDCl_3 and $[\text{D}_6]\text{DMSO}$ were used as solvent using TMS as an internal standard. Chemical shifts are expressed in δ units and ^1H - ^1H and ^1H -C coupling constants in Hz. Fluorescence spectra were recorded on a PerkinElmer LS55 spectrophotometer and UV-vis titration experiments were performed on a JASCO V-630 spectrophotometer.

General method of UV/Vis and fluorescence titration

UV/Vis method

For UV/Vis titrations, a stock solution of the receptor ($10 \mu\text{M}$) was prepared in THF/water (2:3, v/v, at 25°C) using HEPES-buffered solution. The solution of the guest analytes ($2 \times 10^{-4} \text{ M}$) was prepared in deionized water using HEPES buffer at pH 7.1. Solutions of various concentrations containing the probe and increasing concentrations of analytes were prepared separately. The spectra of these solutions were recorded by means of UV-vis method.

Fluorescence method

For fluorescence titrations, stock solution of the probe ($10 \mu\text{M}$) was prepared same as UV-vis titration. The solution of the guest analytes ($2 \times 10^{-4} \text{ M}$) was prepared in deionized water. Solutions of various concentrations containing probe and increasing concentrations of analytes were prepared separately. The spectra of these solutions were recorded by means of fluorescence method.

Synthesis of the probe

(E)-4(4-diphenylamino)styryl)benzaldehyde (0.2 g, 0.53 mmol) was added to a stirred solution of diaminomaleonitrile (0.06 g, 0.53 mmol) in dry ethanol (6 mL). The reaction mixture was refluxed under nitrogen atmosphere for 12 h. The formed brownish-red precipitates were filtered and washed with cold ethanol ($2 \text{ mL} \times 2$). The crude residue was purified by column chromatography (EtOAc/petroleum ether, 1:9) to afford pure probe as a yellow solid (0.2 g). Yield = 80%; m.p. $> 300^\circ\text{C}$ (dec); ^1H NMR (500 MHz, CDCl_3): $\delta = 5.17$ (s, 2H), 7.00 (d, $J = 10 \text{ Hz}$, 1H), 7.06 (t, $J = 7 \text{ Hz}$, 4H), 7.12 (d, $J = 10 \text{ Hz}$, 4H), 7.20 (d, 10 Hz, 1H), 7.28 (d, $J = 10 \text{ Hz}$, 5H), 7.40 (d, $J = 10 \text{ Hz}$, 2H), 7.56 (d, $J = 8 \text{ Hz}$, 1H), 7.79 (d, $J = 10 \text{ Hz}$, 2H), 8.40 ppm (s, 1H); ^{13}C NMR (125 MHz, CDCl_3): $\delta = 108.9$, 112.4, 113.7, 123.2, 123.5, 124.2, 125.0, 125.7, 126.9, 127.9, 129.5, 129.8, 130.6, 131.1, 133.6, 142.2, 147.5, 148.3, 158.7 ppm; HRMS (ESI, positive): calcd. for $\text{C}_{31}\text{H}_{23}\text{N}_5$ $[M]^+$ (m/z): 465.1953; found: 465.4649.

Computational details

DFT calculations were performed using the Gaussian 03 (Revision B.04) package.^[15] "Gauss View" was used for visualization of molecular orbital. The methods used were Becke's three parameter hybrid-exchange functional, the nonlocal correlation provided by

the Lee, Yang, and Parr expression, and the Vosko, Wilk, and Nuair 1980 local correlation functional(III) (B3LYP).^[16] The 6-311 + G(d,p) basis set was used for calculations. Single-point calculations were done in the gas phase. Molecular orbitals were analysed using the AOMix¹⁷ program. All the structures were optimized with B3LYP functional and B3LYP/6-311G + (d,p) basis with no symmetry constrain. Time-dependent DFT calculations were also carried out using the same functional. For these calculations, singlet excited states were calculated based on the singlet ground state geometry.

Method of crystallization

TAM (20 mg) was dissolved in CH₂Cl₂/CH₃CN (1/1, v/v) in a conical flask and it was allowed to stand in a cool place without any perturbation. After three days, diffraction-quality red crystals were separated out and these were collected for X-ray crystallographic analysis.

Cell biological study

Venous blood (3 mL) was obtained from volunteer donors (age > 50 years) with their informed consent. Peripheral blood mononuclear cells (PBMCs) were isolated by density gradient centrifugation using histopaque-1077 obtained from SIGMA. PBMCs were washed and suspended in PBS and divided into two sets. In one set, 20 μM of NaOCl solution was added as a source of OCl⁻. TAM samples were prepared in PBS buffer. Both the PBMCs samples (with and without OCl⁻) were separately incubated with 10 μM of TAM solution for 15 min at 37 °C. Finally, the cells were observed under a confocal fluorescence microscope (Olympus IX81 microscope) using fluorescence emissions at green channel (490–550 nm) and red channel (620–650 nm), respectively.

Acknowledgements

Authors thank CSIR and DST, Govt of India for financial supports. S.D., K.A., B.P., K.G. acknowledge CSIR for providing them fellowship. CKQ and HKF thank Malaysian Government and USM for Research University Individual Grant (Synthesis, Characterization And Nonlinear Optical Properties Of Novel Chalcone Compounds) and Fundamental Research Grant Scheme (FRGS) (203/PFIZIK/6711411). The authors extend their appreciation to The Deanship of Scientific Research at King Saud University for funding the work through the research group project no. RGPVPP-207. Authors like to acknowledge CU-DBT-IPLS for confocal fluorescence microscope facility. S.S likes to acknowledge DST for Ramanna Fellowship.

Keywords: blood-cell imaging · fluorescent probes · hypochlorite · ratiometric · sensors · solvatofluorochromism

- [1] A. Gomes, E. Fernandes, J. L. F. C. Lima, *J. Biochem. Biophys. Methods* **2005**, *65*, 45–80.
 [2] J. Shepherd, S. A. Hilderbrand, P. Wateman, J. W. Heinecke, R. Weissleder, P. Libby, *Chem. Biol.* **2007**, *14*, 1221.
 [3] a) Y. Kawai, Y. Matsui, H. Kondo, H. Morinaga, K. Uchida, N. Miyoshi, Y. Nakamura, T. Osawa, *Chem. Res. Toxicol.* **2008**, *21*, 1407; b) Y. W. Yap, M. Whiteman, N. S. Cheung, *Cell. Signalling* **2007**, *19*, 219; c) Y. W. Yap, M. Whiteman, B. H. Bay, Y. Li, F. S. Sheu, R. Z. Qi, C. H. Tan, N. S. Cheung, *J. Neurochem.* **2006**, *98*, 1597–1609.

- [4] M. J. Davies, *J. Clin. Biochem. Nutr.* **2011**, *48*, 8.
 [5] M. J. Steinbeck, L. J. Nesti, P. F. Sharkey, J. Parvizi, *J. Orthop. Res.* **2007**, *25*, 1128.
 [6] L. C. Adam, G. Gordon, *Anal. Chem.* **1995**, *67*, 535.
 [7] K. C. Huang, C. C. Yang, K. T. Lee, C. T. Chien, *Kidney Int.* **2003**, *64*, 704.
 [8] S. Hammerschmidt, N. Büchler, H. Wahn, *Chest* **2002**, *121*, 573–581.
 [9] Y. Maruyama, B. Lindholm, P. Stenvinkel, *J. Nephrol.* **2004**, *17*, S72–S76.
 [10] a) X. Chen, K.-A. Lee, E.-M. Ha, K. M. Lee, J. Yoon, *Chem. Commun.* **2011**, *47*, 4373; b) X. Chen, X. Tian, I. Shin, J. Yoon, *Chem. Soc. Rev.* **2011**, *40*, 4783; c) T.-I. Kim, S. Park, Y. Choi, Y. Kim, *Chem. Asian J.* **2011**, *6*, 1358; d) X. Q. Chen, X. Wang, S. Wang, W. Shi, K. Wang, H. M. Ma, *Chem. Eur. J.* **2008**, *14*, 4719; e) S. Kenmoku, Y. Urano, H. Kojima, T. Nagano, *J. Am. Chem. Soc.* **2007**, *129*, 7313; f) Y. Koide, Y. Urano, K. Hanaoka, T. Terai, T. Nagano, *J. Am. Chem. Soc.* **2011**, *133*, 5680; g) S. Goswami, S. Das, K. Aich, P. K. Nandi, K. Ghoshal, C. K. Quah, M. Bhattacharyya, H.-K. Fun, H. A. Abdel-Aziz, *RSC Adv.* **2014**, *4*, 24881; h) B. Wang, P. Li, F. Yu, P. Song, X. Sun, S. Yang, Z. Lou, K. Han, *Chem. Commun.* **2013**, *49*, 1014; i) G. Li, D. Zhu, Q. Liu, L. Xue, H. Jiang, *Org. Lett.* **2013**, *15*, 2002; j) T. Guo, L. Cui, J. Shen, R. Wang, W. Zhu, Y. Xu, X. Qian, *Chem. Commun.* **2013**, *49*, 1862; k) L. Yuan, W. Lin, J. Song, Y. Yang, *Chem. Commun.* **2011**, *47*, 12691; l) J. J. Hu, N.-K. Wong, Q. Gu, X. Bai, S. Ye, D. Yang, *Org. Lett.* **2014**, *16*, 3544; m) J.-T. Hou, M.-Y. Wu, K. Li, J. Yang, K.-K. Yu, Y.-M. Xie, X.-Q. Yu, *Chem. Commun.* **2014**, *50*, 8640; n) Q. Xu, K.-A. Lee, S. Lee, K. M. Lee, W.-J. Lee, J. Yoon, *J. Am. Chem. Soc.* **2013**, *135*, 9944.
 [11] O. S. Wolfbeis, *Angew. Chem. Int. Ed.* **2013**, *52*, 9864; *Angew. Chem.* **2013**, *125*, 10048.
 [12] a) S. Goswami, S. Das, K. Aich, *Tetrahedron Lett.* **2013**, *54*, 4620; b) S. Goswami, S. Das, K. Aich, D. Sarkar, T. K. Mondal, *Tetrahedron Lett.* **2013**, *54*, 6892; c) S. Goswami, K. Aich, S. Das, S. B. Roy, B. Pakhira, S. Sarkar, *RSC Adv.* **2014**, *4*, 14210; d) S. Goswami, K. Aich, D. Sen, *Chem. Lett.* **2012**, *41*, 863; e) S. Goswami, S. Das, K. Aich, D. Sarkar, T. K. Mondal, *Tetrahedron Lett.* **2014**, *55*, 2695; f) S. Goswami, K. Aich, S. Das, A. K. Das, A. Manna, S. Halder, *Analyst* **2013**, *138*, 1903; g) S. Goswami, S. Das, K. Aich, D. Sarkar, T. K. Mondal, C. K. Quah, H.-K. Fun, *Dalton Trans.* **2013**, *42*, 15113; h) S. Goswami, K. Aich, S. Das, A. K. Das, D. Sarkar, S. Panja, T. K. Mondal, S. K. Mukhopadhyay, *Chem. Commun.* **2013**, *49*, 10739; i) S. Goswami, S. Das, K. Aich, B. Pakhira, S. Panja, S. K. Mukherjee, S. Sarkar, *Org. Lett.* **2013**, *15*, 5412.
 [13] Y.-D. Lin, Y.-S. Peng, W. Su, C.-H. Tu, C.-H. Sun, T. J. Chow, *Tetrahedron* **2012**, *68*, 2523.
 [14] a) M. Shortreed, R. Kopelman, M. Kuhn, B. Hoyland, *Anal. Chem.* **1996**, *68*, 1414; b) W. Lin, L. Yuan, Z. Cao, Y. Feng, L. Long, *Chem. Eur. J.* **2009**, *15*, 5096.
 [15] Gaussian 03, Revision B.04, M. J. Frisch, G. W. Trucks, H. B. Schlegel, G. E. Scuseria, M. A. Robb, J. R. Cheeseman, Jr., J. A. Montgomery, T. Vreven, K. N. Kudin, J. C. Burant, J. M. Millam, S. S. Iyengar, J. Tomasi, V. Barone, B. Mennucci, M. Cossi, G. Scalmani, N. Rega, G. A. Petersson, H. Nakatsuji, M. Hada, M. Ehara, K. Toyota, R. Fukuda, J. Hasegawa, M. Ishida, T. Nakajima, Y. Honda, O. Kitao, H. Nakai, M. Klene, X. Li, J. E. Knox, H. P. Hratchian, J. B. Cross, V. Bakken, C. Adamo, J. Jaramillo, R. Gomperts, R. E. Stratmann, O. Yazyev, A. J. Austin, R. Cammi, C. Pomelli, J. W. Ochterski, P. Y. Ayala, K. Morokuma, G. A. Voth, P. Salvador, J. J. Dannenberg, V. G. Zakrzewski, S. Dapprich, A. D. Daniels, M. C. Strain, O. Farkas, D. K. Malick, A. D. Rabuck, K. Raghavachari, K. Foresman, J. V. Ortiz, Q. Cui, A. G. Baboul, S. Clifford, J. Cioslowski, B. B. Stefanov, G. Liu, A. Liashenko, P. Piskorz, I. Komaromi, R. L. Martin, D. J. Fox, T. Keith, M. A. Al-Laham, C. Y. Peng, A. Nanayakkara, M. Challacombe, P. M. W. Gill, B. Johnson, W. Chen, M. W. Wong, C. Gonzalez, J. A. Pople, Gaussian, Inc., Pittsburgh, PA, **2003**.
 [16] a) A. D. Becke, *J. Chem. Phys.* **1993**, *98*, 5648; b) C. Lee, W. Yang, R. G. Parr, *Phys. Rev. B* **1988**, *37*, 785.
 [17] a) S. I. Gorelsky, AOMix, Program for Molecular Orbital Analysis, University of Ottawa, Ottawa, **2007**, <http://www.sg-chem.net/>; b) S. I. Gorelsky, A. B. P. Lever, *J. Organomet. Chem.* **2001**, *635*, 187.

Received: October 30, 2014

Revised: December 3, 2014

Published online on ■■■■■ 0000

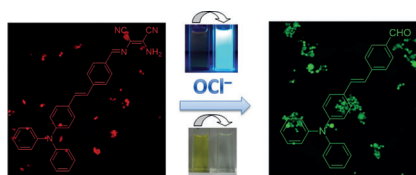
FULL PAPER

Sensors

Shyamaprosad Goswami,*
Krishnendu Aich, Sangita Das,
Bholanath Pakhira, Kakali Ghoshal,
Ching Kheng Quah,
Maitree Bhattacharyya, Hoong-Kun Fun,
Sabyasachi Sarkar



 **A Triphenyl Amine-Based Solvatofluorochromic Dye for the Selective and Ratiometric Sensing of OCl^- in Human Blood Cells**



Green means danger! A new triphenyl amine-diaminomaleonitrile-based probe was synthesized. This probe acts as a polarity probe with a strong positive emission solvatofluorochromism. It exclusively detects OCl^- in a ratiometric manner in a mixed aqueous system with a detection limit of about 10^{-8} M. Moreover, it can detect OCl^- in vivo in human blood cells.